Clim Dyn (2013) 41:2921–2936
DOI 10.1007/s00382-012-1644-1

Present-day and future Amazonian precipitation in global climate models: CMIP5 versus CMIP3

E. Joetzjer · H. Douville · C. Delire · P. Ciais

Received: 27 July 2012 / Accepted: 18 December 2012 / Published online: 23 January 2013

Abstract The present study aims at evaluating and comparing precipitation over the Amazon in two sets of historical and future climate simulations based on phase 3 (CMIP3) and 5 (CMIP5) of the Coupled Model Intercomparison Project. Thirteen models have been selected in order to discuss (1) potential improvements in the simulation of present-day climate and (2) the potential reduction in the uncertainties of the model response to increasing concentrations of greenhouse gases. While several features of present-day precipitation—including annual cycle, spatial distribution and co variability with tropical sea surface temperature (SST)—have been improved, strong uncertainties remain in the climate projections. A closer comparison between CMIP5 and CMIP3 highlights a weaker consensus on increased precipitation during the wet season, but a stronger consensus on a drying and lengthening of the dry season. The latter response is related to a northward shift of the boreal summer intertropical convergence zone in CMIP5, in line with a more asymmetric warming between the northern and southern hemispheres. The large uncertainties that persist in the rainfall response arise from contrasted anomalies in both moisture convergence and evapotranspiration. They might be related to the diverse response of tropical SST and ENSO (El Niño Southern Oscillation) variability, as well as to spurious behaviours among the models that show the most extreme response. Model improvements of present-day climate do not necessarily translate into more reliable projections and further efforts are needed for constraining the pattern of the SST response and the soil moisture feedback in global climate scenarios.

Keywords CMIP · Amazonian precipitation · Model evaluation · Climate change · Uncertainties

1 Introduction

The Amazon watershed is the largest on Earth. It carries about 20 % of global freshwater discharge and the tropical forest accounts for 10 % of the world's terrestrial productivity and biomass. Thus, the Amazon plays an important role in global climate, regulating global water and carbon cycles (Foley 2002). Considering Amazon ecosystem relevance to global climate, the severe droughts that have impacted the basin this last decade are of great concern. Phillips et al. (2009) showed that the 2005 drought resulted in a loss of forest biomass, through enhanced tree mortality and growth decline, therefore reducing the large long-term carbon sink. In 2010, an even more severe drought occurred, as indicated by record low river levels in the last century (Xu et al. 2011). The rainforest was strongly affected, and a widespread loss of photosynthetic capacity was observed among the major part of the basin (Xu et al. 2011), again reducing the carbon sink role of the Amazonian ecosystem during these particular events (Lewis et al. 2011; Potter et al. 2011).

Precipitation over the Amazon shows a strong spatio-temporal variability on a wide range of scales. The annual cycle is dominated by the seasonal migration of the intertropical convergence zone (ITCZ). Interannual variations are mainly driven by SST anomalies over the surrounding

E. Joetzjer (✉) · H. Douville · C. Delire
CNRM-GAME, 42 avenue G. Coriolis, 31057 Toulouse, France
e-mail: emilie.joetzjer@meteo.fr

P. Ciais
Laboratory of Climate Sciences and the Environment, L'Orme des Merisiers, 91191 Gif-sur-Yvette, France

oceans. In particular, a close relationship between ENSO and Amazonian precipitation is widely recognized in the community (Richey et al. 1989; Marengo 1992; Meggers 1994; Uvo et al. 1998; Botta et al. 2002; Foley 2002; Li et al. 2011). However, the 2005 drought was driven not only by El Niño, as is often the case, but mainly by unusually warm tropical North Atlantic (hereafter TNA) SSTs (Marengo et al. 2008, Zeng et al. 2008, Yoon and Zeng 2009). The implication of the TNA was also suspected for triggering the 2010 event (Marengo et al. 2011; Lewis et al. 2011). The southern tropical Atlantic was also highlighted as a potential source of rainfall interannual variability (Yoon and Zeng 2009), but its influence is mainly found during the wet-to-dry transition season and will not be discussed hereafter. Similarly, the influence of the North Atlantic SST on rainfall multidecadal variability (Marengo 2004) will not be assessed given the limited time series and the focus on the late twentieth and twenty-first centuries (rather than on the transient precipitation response) in the present study.

On climate change timescales, tropical SST patterns and related anomalies in large-scale moisture transport are not the only source of variability in precipitation over the Amazon. As emphasized by Seager et al. (2010), changes in moisture convergence (i.e. precipitation minus evaporation) are "thermodynamically mediated" rather than dynamically driven. They are partly explained by increased specific humidity in a warmer climate and are therefore dependent on the magnitude of the simulated global warming. Moreover, changes in land surface evapotranspiration are also expected (Douville et al. 2012), not only as a response of the surface energy budget to increasing radiative forcings, but also as a consequence of potential land surface feedbacks related to physiological and biophysical processes (Sellers et al. 1996; Foley et al. 2003; Betts et al. 2004; Marengo et al. 2008).

The fourth Assessment Report of the Intergovernmental Panel on Climate Change (IPCC AR4) was based upon simulations from the phase 3 of the coupled model intercomparison project (CMIP3). CMIP3 models show deficiencies in simulating present-day precipitation over the Amazon and its inter-annual variability (Vera et al. 2006; Dai 2006; Rojas et al. 2006; Malhi et al. 2009). Above all, they tend to underestimate current precipitation averaged over the basin, partly due to the low resolution hampering models to represent finer-scale meteorological processes that are known to intensify precipitation (Malhi et al. 2009). Besides horizontal resolution, deficiencies in the physical parameterizations such as deep convection or land surface hydrology can also contribute to precipitation biases and associated errors in large scale circulation (e.g. Richter et al. 2012).

In climate scenarios, CMIP3 models disagree on the fate of Amazon precipitation at the end of the 21st century. Across a subset of 11 models analysed by Li et al. (2006) under the "middle road" concentration scenario A1B, five out of eleven models predicted increased precipitation, three no change in annual mean rainfall, and three projected a drier climate. Similar discrepancies were found by Malhi et al. (2008) among 19 models under the more severe scenario A2. More recently, Cook et al. (2012) analysed the scenario A1B outputs of 24 models and found a possible (but not systematic) decline of the dry season precipitation in southern Amazonia even if rainfall in the core of the Amazon basin was projected to increase in nearly all models.

Therefore and so far, in the light of CMIP3, the future of precipitation over the Amazon remains strongly model-dependent. There is even more uncertainties considering that most CMIP3 models did not include some of the biogeochemical feedbacks at play in the Amazon (Rammig et al. 2010). Recent studies suggested that including them could result in a drier Amazon at the end of the twenty-first century (Betts et al. 2004; Malhi et al. 2009). One model even predicted a possible "dieback" of the Amazonian rainforest, which turned from a net sink to a net source of CO_2 by the end of the twenty-first century, thereby reinforcing global warming and a regional decrease in precipitation (Cox et al. 2000, 2004). These results should however be considered with caution (e.g. Cook et al. 2012) and a more recent version of the same model predicts little change in the rainforest extent (Good et al. 2012).

In the perspective of the fifth Assessment Report of IPCC, it is timely to compare CMIP5 with CMIP3 models for both present-day (historical simulations) and future climates (RCP8.5 versus SRES-A2 concentration scenarios) and address the following questions: (1) Is there any improvement in the models ability to capture present-day precipitation in terms of mean annual cycle, spatial distribution and inter-annual variability?, (2) Is there any change in the models response to climate change and any reduction in the associated uncertainties?

Section 2 describes the observed data, the statistical methods and the coupled climate models chosen in both CMIP3 and CMIP5. Section 3 first evaluates historical simulations of precipitation over the Amazon in terms of mean annual cycle, spatial distribution and inter-annual variability. It also compares the simulated response to climate change. Results are further discussed in Sect. 4 which provides preliminary explanations for the spread in the multi-model projections. The main conclusions are summarized in Sect. 5.

2 Data and methods

2.1 Data

The Global Precipitation Climatology Center dataset (Rudolf et al. 2011) and the Hadley Centre HadSST

monthly SST climatology (Rayner et al. 2003), both provided at the 1° resolution for the 1901–2009 period, were used in this study. A subset of 13 models were chosen among those developed by internationally recognized research institutes that contributed to both inter-comparisons and had already released their CMIP5 outputs (http://cmip-pcmdi.llnl.gov/cmip5//) at the beginning of the present study. Description and references for each model are given in Table 1. While most CMIP3 models did not account for potential carbon cycle feedbacks from vegetation and soil, an attempt has been made to select as many earth system models as possible in CMIP5, including from the research institutes that had provided both coupled and uncoupled simulations.

For both CMIP intercomparisons, rainfall projections are here based on the most severe greenhouse gas concentration scenario in order to maximize the signal to noise ratio and use a single integration for each model. For CMIP3, this was the scenario A2 proposed by the IPCC Special Report on Emission Scenario (SRES) in which CO_2 concentration reaches about 840 ppm at the end of the twenty-first century and the radiative forcing increases by 7 W/m^2 (Riahi et al. 2007). To be consistent, we chose for CMIP5 simulations the Representative Concentration Pathways (RCP) 8.5 which is based upon the revised and extended storyline of the scenario A2 and characterized by a rising radiative forcing pathway leading to 8.5 W/m^2 (and about 940 ppm of CO_2) in 2100 (Riahi et al. 2011). More idealized CMIP simulations based on a 1 % increase of CO_2 concentration until four times CO_2 were also considered in order to get rid of differences between the SRES-A2 and RCP8.5 concentration scenarios. It will be thus possible to attribute differences between CMIP3 and CMIP5 climate projections to changes in models rather than in scenarios. Such experiments are also useful to isolate the possible influence of anthropogenic aerosols in the CMIP5 RCP8.5 projections. Note that for CMIP3, only 11 out of the selected 13 models have participated in the 1 % CO_2 experiment. Comparison between CMIP5 and CMIP3 in this respect will be based on these 11 models only.

2.2 Methods

We focus our attention to the region outlined by the black square in Fig. 1. The present-day climatology was established for the 1971–2000 period on the native grid of each individual model. The ensemble mean for each CMIP exercise (hereafter multi-model) was calculated after a bilinear interpolation on a common 64 × 128 horizontal grid, i.e. a medium (low) horizontal resolution compared to the range in CMIP3 (CMIP5). The same treatment was applied for the late twenty-first century climatology and climate change was estimated as the difference between 2071–2100 and 1971–2000, respectively. In the idealized 1 % CO_2 experiments, climate change was simply diagnosed as the difference between two 30-year time slices chosen as years 11–40 and years 111–140 respectively, which roughly corresponds to the same global warming as in the scenarios. Better surrogates of both present-day and future climate could be defined in such idealized experiments, using periods with equivalent greenhouse gas radiative forcing rather than approximatively equivalent global mean temperature, but this would not change our conclusions about the nature of the

Table 1 List of CMIP3 and CMIP5 models used in this study

Short name	Originating group(s)	Model version CMIP3	Atmospheric resolution CMIP3	Model version CMIP5	Atmospheric resolution CMIP5
CCCMA	CCCMA (Victoria, Canada)	cccma-cgcm3-1	96 × 48, L31	canesm2	128 × 64, L35
CNRM	CNRM & CERFACS (Toulouse, France)	cnrm-cm3	128 × 64, L45	cnrm-cm5	256 × 128, L31
CSIRO	CSIRO & QCCCE (Australia)	csiro-mk3-0[a]	192 × 96, L18	csiro-mk3-6-0	192 × 96, L18
GFDL	NOAA-GFDL (Princeton, USA)	gfdl-cm2-0	144 × 90, L24	gfdl-esm2 m	144 × 90, L24
GISS	NASA-GISS (New York, USA)	giss-model-e-r	72 × 46, L20	giss-e2-r	144 × 90, L40
INM	INM (Moscow, Russia)	inmcm3-0[a]	72 × 45, L33	inmcm4	180 × 120, L21
IPSL	IPSL (Paris, France)	ipsl-cm4-v1	96 × 72, L19	ipsl-sm5a-lr	96 × 96, L39
MIROC	AORI & NIES & JAMSTEC (Japan)	miroc-3.2	128 × 64, L20	miroc-esm	128 × 64, L35
MOHC	MOHC (Exeter, UK)	hadgem1	192 × 145, L38	hadgem2-es	192 × 145, L38
MPI	MPIM (Hamburg, Germany)	mpi-echam5	192 × 96, L32	mpi-esm-lr	192 × 96, L47
MRI	MRI (Tsukuba, Japan)	mri-cgcm2-3-2a	128 × 64, L30	mri-cgcm3	320 × 160, L48
NCAR	NCAR (Boulder, USA)	ccsm3	256 × 128, L26	ccsm4	288 × 192, L26
NCC	NCC (Oslo, Norway)	bccr-bcm2.0	128 × 64, L31	noresm1-m	144 × 96, L26

[a] Models that have no outputs available for the idealized 1 % CO_2 experiments

differences between the CMIP3 and CMIP5 scenarios. Besides annual means, seasonal means have also been computed to highlight contrasted behaviours between the dry season (June to September, hereafter JJAS), and the wet season (December to March, hereafter DJFM). Note that a more objective definition of dry versus wet season would have required daily instead of monthly model outputs and is beyond the scope of the present study. Nevertheless, projected changes in the length of the dry season will be briefly discussed in Sect. 3.2 using monthly data and an empirical threshold of 100 mm/month (Sombroek 2001) for precipitation averaged over the whole Amazonian region.

Focusing on inter-annual variability of precipitation requires removal of the low-frequency variability in both observed and simulated raw data. To achieve this objective, we used a digital high-pass filter (Wallace et al. 1988) (hereafter HPF) with a cut-off of 10 years, in order to separate the multi-decadal (low frequency) from the inter-annual (high frequency) timescales. The HPF was applied at each grid point on the observed SST and precipitation for a Maximum Covariance Analysis (MCA) (Fig. 3) and onto regional (i.e. spatially averaged) climate indices for the evaluation of rainfall variability in CMIP simulations against observations (Fig. 4).

The MCA, also called Singular Value of Decomposition (SVD) (Bretherton et al. 1992; Wallace et al. 1992) was performed between high-pass filtered annual mean global SST and high-pass filtered annual mean precipitation over northern South America (Fig. 3). It can be seen as a generalization of the principal component analysis (PCA) and it is here applied to identify pairs of coupled spatial patterns that maximize the covariance between global SST and regional precipitation. This brief analysis of the observed interannual variability provides the basis for a synthetic evaluation of the simulated teleconnections between the Amazonian precipitation and the Pacific or Atlantic tropical ocean. A more detailed analysis based on the MCA applied on each individual model and/or on seasonal rather than annual mean fields is beyond the scope of the present study.

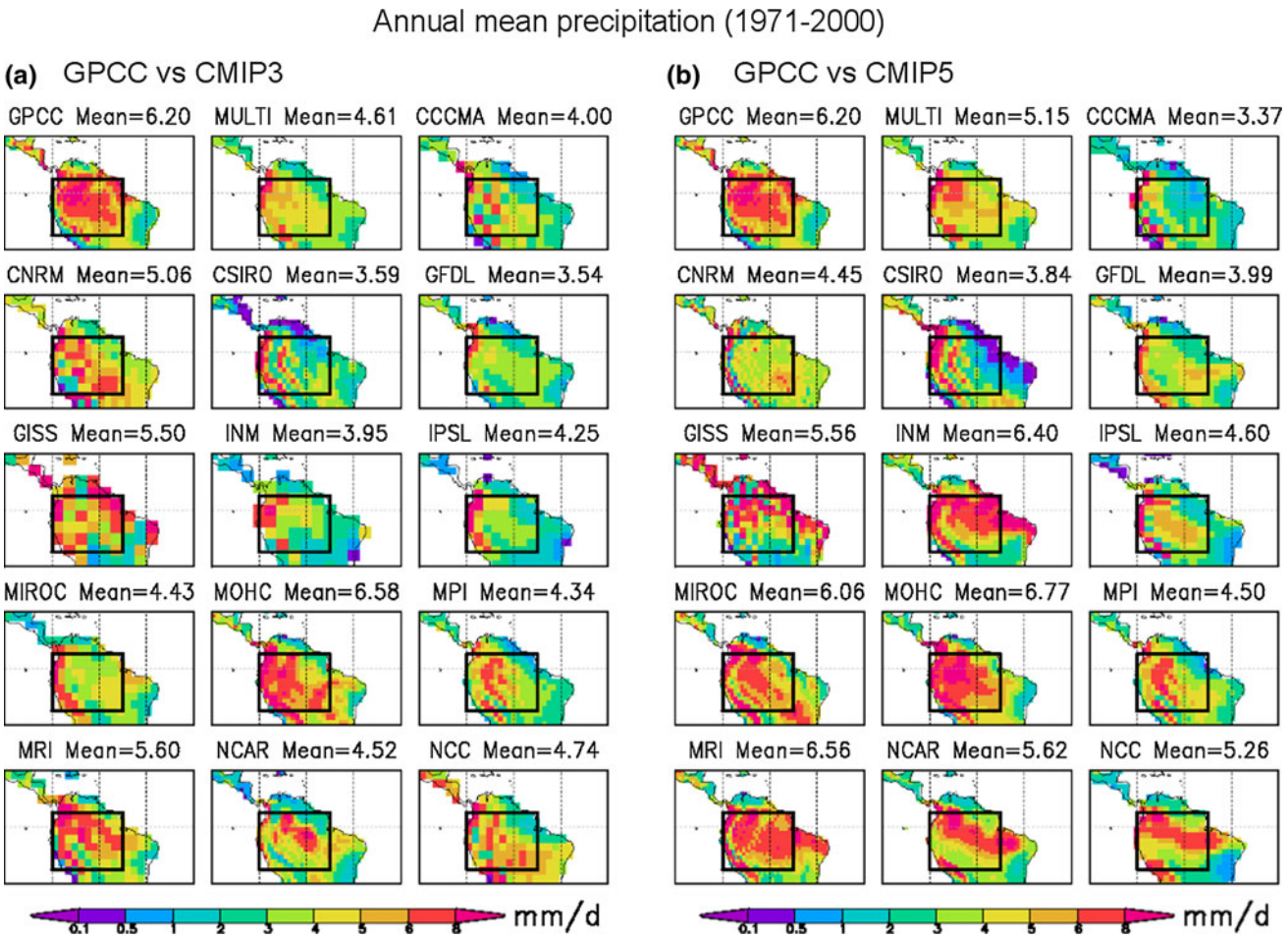

Fig. 1 Spatial distribution of climatological (1971–2000) annual mean precipitation (mm/day) in **a** CMIP3 and **b** CMIP5 models (see Table 1) versus the observed GPCC climatology (*top left* panel in both **a**, **b**). The average of all the models (MULTI) is shown *left* of the GPCC data

3 Results

3.1 Present-day climate

The spatial distribution of the observed annual mean precipitation (Fig. 1) shows an average rainfall of 6.2 mm/day over the selected area. However, precipitation is unevenly distributed within the box, with high precipitation (above 6 mm/day) over the central part of the basin and along the eastern slopes of the Andes and less precipitation in the southern and eastern part of the domain. Looking at the CMIP3 ensemble mean climatology (Fig. 1a), the multi-model mean shows a pronounced dry bias. Such a bias is found in most models (except MOHC) and does not seem related to the variable horizontal resolution of the atmospheric models. However, the lack of high resolution is obviously a limitation for capturing the pattern of the precipitation climatology and particularly the orographic influence of the Andes in western Amazonia.

As revealed by the multi-model climatology (interpolated on the same horizontal grid as the CMIP3 multi-model), CMIP5 shows a reduction in the annual and areal mean dry bias. Such an improvement is found in all models except CNRM and CCCMA. While some models (e.g. INM or MIROC) also show improved precipitation patterns with increasing resolution, many model share common biases between CMIP3 and CMIP5. The main exception is NCC which is the only model whose atmospheric and land surface components have been changed rather than upgraded between CMIP3 and CMIP5. In the NCC model, the ARPEGE-Climat AGCM from CNRM has been replaced by the CAM4 AGCM from NCAR. Such a change is easily tractable in the precipitation climatology and suggests a strong influence of the atmosphere and/or land surface components on precipitation biases in coupled ocean–atmosphere GCMs.

Figure 2 focuses on the mean annual cycle of monthly precipitation averaged over the Amazonian domain (i.e. within the black domain in Fig. 1). The multi-model reduction in the annual mean dry bias between CMIP3 and CMIP5 is mainly due to increased precipitation during the wet season (DJFM). Dry season (JJAS) precipitation remains strongly underestimated. Moreover the multi-model spread (±1 standard deviation) and envelope (minimum vs maximum values) have not been reduced, thereby confirming that most models still have serious difficulties in simulating present-day seasonal precipitation over the Amazon basin.

Besides a realistic present-day climatology, a prerequisite to reliable climate scenarios is also a reasonable representation of interannual variability. Interannual variability of precipitation over the Amazon has been linked to variations of SST over the surrounding tropical oceans. In order to summarize the observed teleconnections over the 1901–2009 period, a MCA was applied between observed annual mean HPF precipitation over northern South America and observed annual mean HPF SST over the global ocean.

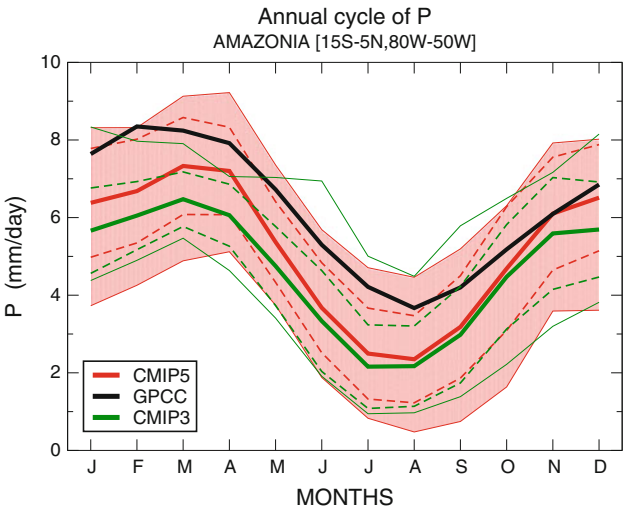

Fig. 2 Climatological CMIP5, CMIP3 and observed (GPCC) mean annual cycle of monthly precipitation (mm/day) over Amazonia: multi-model ensemble mean (*thick lines*) ± 1 standard deviation (*dashed lines*), as well as extreme values (*thin lines*)

The first mode (Fig. 3) mainly links precipitation over the eastern Amazon basin and SSTs in the equatorial Pacific. The SST pattern shows a strong negative anomaly over the Equator surrounded by two positives anomalies, which is characteristic of the cold phase of ENSO. This pattern is associated to positive precipitation anomalies over the Amazon basin. It is even more obvious when DJFM (rather than annual) mean data are considered (not shown), in line with the annual cycle of ENSO variability, but the signal is also found beyond the DJFM season in line with the persistence of ENSO anomalies and the possible recycling of precipitation after the wet season through a soil moisture—precipitation feedback.

The second mode explains a weaker fraction of the annual precipitation variability and suggests a link with the TNA SST. It associates a warm anomaly over the TNA to a deficit of precipitation on the eastern part and to more precipitation over central America. The signal is strongest during the dry season (Yoon and Zeng 2009) and is not totally independent from ENSO variability as suggested by the concomitant weak SST signal found in the equatorial Pacific (Fig. 3).

This MCA analysis clearly shows the observed dominant links between Amazonian rainfall and SSTs over both tropical Pacific and tropical Atlantic at inter-annual timescales. It indicates a strong influence of ENSO, while the causality of the relationship with the TNA is less clear. If

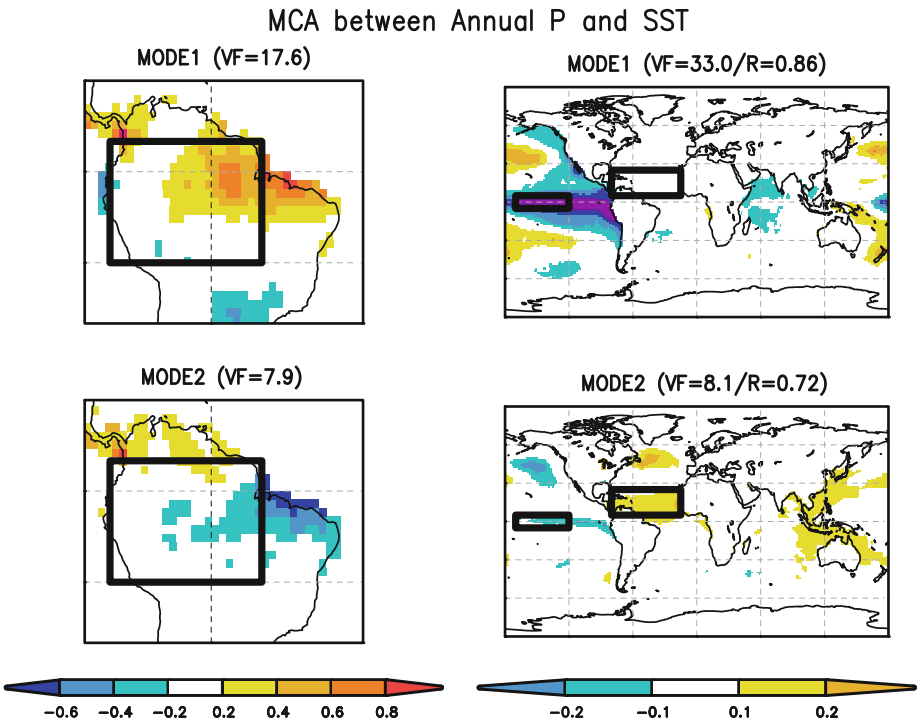

Fig. 3 First two modes of a maximum covariance analysis between observed annual mean precipitation over Amazonia and observed annual mean SST (HadSST) over the global ocean based on high-pass filtered time series over the whole twentieth century: homogeneous vectors of precipitation (*left panels*) and homogeneous vectors of SST (*right panels*). VF denotes the explained fraction of variance and R the temporal correlation between precipitation and SST expansion coefficients

the influence of the Pacific is broadly accepted, the role of the TNA in inter-annual variability of precipitation has been highlighted more recently. Nevertheless, Yoon and Zeng (2009) showed that removing ENSO from North Atlantic SST via linear regression resolves this causality problem in that the residual Atlantic variability correlates well and is in phase with the Amazon rainfall. Therefore, this link will also be evaluated in the present study.

For the sake of brevity, we don't apply the MCA on each model simulations. The model evaluation is conducted on the basis of lead/lag correlations between annual mean precipitation time series averaged over the whole Amazonian domain and monthly mean SST anomalies averaged over the Niño3-4 and TNA domains respectively (also shown as black rectangles in Fig. 3). The results are summarized in Fig. 4. From 6 months (July, year-1) before an anomalously dry (wet) year until August of that year (year 0), there is a strong negative correlation between Nino3.4 SSTs and year 0 annual mean precipitation, indicating that warm (cold) SST anomalies tend to precede a dry (wet) year in Amazonia. This is the well known El Niño/wet season drought link. Similar results were also found by Zeng (1999), who showed that monthly precipitation lagged monthly Nino3.4 SST by 3–4 months. Figure 4a also suggests a positive correlation with warm (cold) SSTs leading by 12–9 months a dry (wet) year in Amazonia. The correlation is however weaker and could simply reflect the 2 to 3-year peak of ENSO variability.

The signal is different for the TNA box. It starts with a weak but significant positive correlation when SSTs are leading rainfall anomalies by 10–3 months. The correlation then changes sign with warm TNA SSTs linked to a drought during the anomalous rainfall year. Hence both observed monthly Nino3.4 and TNA SSTs are significantly anti-correlated with Amazon precipitation during the drought (wet) year, in line with the results shown in Fig. 3.

There is a remarkable improvement in the way the coupled climate models represent these relationships for both locations between CMIP3 and CMIP5. On average, the CMIP5 models represent fairly well the magnitude of the correlation and the timing of the sign change. This was much less the case for CMIP3 models. The spread between the different models is also greatly reduced with all the models now simulating a drought when SSTs are high. For both SST forcing locations, simulations from CMIP5 capture the link between precipitation and SST and outperform the results from CMIP3.

3.2 Climate change scenarios

Climate change is here estimated either as the difference between 1971–2000 and 2071–2100 using the historical simulations and the SRES-A2 or RCP8.5 climate scenarios (default) or as the difference between years 11–40 and years 111–140 using the idealized 1 % CO_2 experiments. Starting with the climate scenarios, Fig. 5a shows the absolute anomalies of the mean annual cycle of monthly precipitation. "Anomalies" describe the difference between future and present-day simulation. Both multi-model ensemble means indicate an increase in the amplitude of the seasonal cycle of precipitation at the end of the

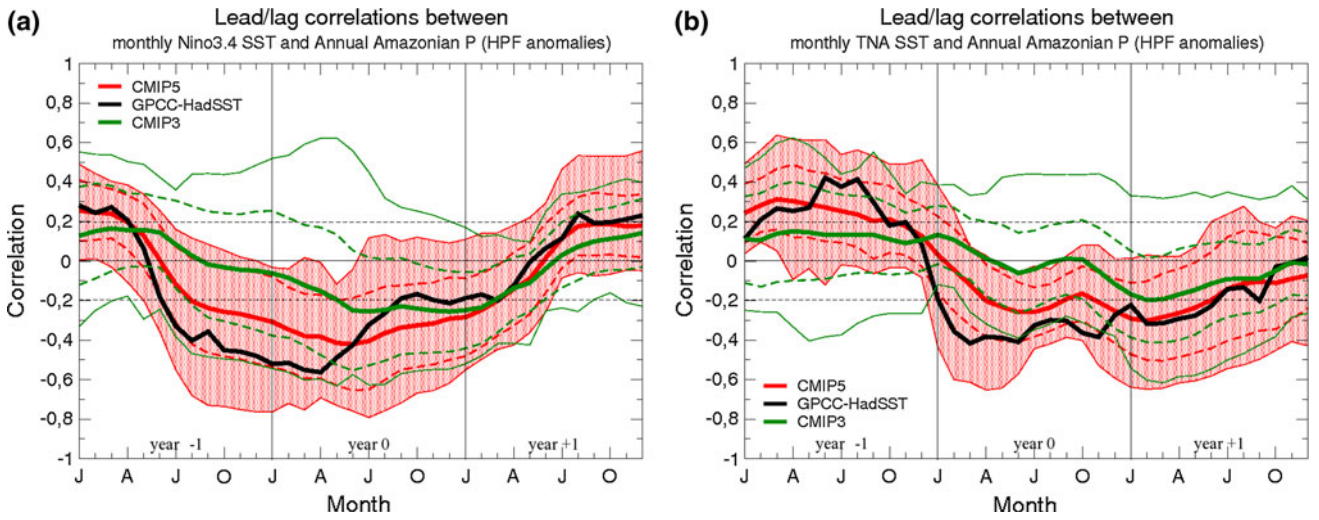

Fig. 4 Twentieth century lead-lag correlations between annual mean Amazonian precipitation and monthly SSTs in the observations (GPCC and HadSST), CMIP5 vs CMIP3 models averaged over **a** the Nino3.4, and **b** the Tropical North Atlantic *boxes*. Precipitation averaged over the *box* defined in Fig. 1. And Nino3.4 and Tropical North Atlantic boxes defined in Fig. 3

twenty-first century, with a drier dry season and a slightly wetter wet season. CMIP5 indicates a weaker increase in the wet season precipitation than the one projected by CMIP3, but the dry season drying appears more intense and persistent. This relatively robust feature is confirmed by simple statistics about the length of the dry season, here defined by the number of months with rainfall less than 100 mm/month (Sombroek 2001). Most CMIP5 models project a significant lengthening with an ensemble mean increase of about 2 weeks (Table 2a), in qualitative agreement with the results of Cook et al. (2012) based on the former generation SRES-A1B climate scenarios. The chosen precipitation threshold is somewhat arbitrary and corresponds to a dry season of 1 month in the observed data. Note that varying it from ±20 % leads to similar results. Besides, taking a relative threshold (here the number of months with precipitation below the 10th percentile calculated over 1901–2009) also leads to a significant lengthening of the dry season in CMIP5 simulations (Table 2b). However, a unique precipitation threshold is not necessarily relevant for future climate since the length of the dry season might also being monitored by other variables as evapotranspiration (Joetzjer et al. 2012), which is beyond the scope of this present study.

Beyond the ensemble mean behaviour, there remains large uncertainties within the subset of selected models, even about the sign of the basin-scale precipitation change. Model spread has not been systematically reduced from CMIP3 to CMIP5 and there is still no clear response to the prescribed radiative forcings. Note that the RCP8.5 greenhouse gas concentration scenario is slightly more severe that the A2 scenario, which could partly explain the increasing severity of the dry season in CMIP5. This hypothesis is not confirmed by Fig. 5b showing the results of the idealized 1 %CO_2 experiments. In this case and despite identical radiative forcings, CMIP5 models still show a significant drying and lengthening of the dry season, while there is no such evidence in CMIP3 models when precipitation is averaged over the whole Amazonian domain.

Moving back to the scenarios, the spatial distribution of the seasonal mean precipitation anomalies has also changed between CMIP3 and CMIP5. Left panels in Fig. 6 show the model consensus defined as the percentage of models in agreement with the sign of the multi-model mean while right panels show the pattern of the ensemble mean anomalies. Note that the percentage is here estimated among a subset of only 13 models. It should be thus taken with caution and, though widely used in the IPCC AR4, this measure of consensus does not account for the full distribution of the models (Power et al. 2012). Despite the use of a different (A2 instead of A1B) concentration scenario and of a reduced (13 instead of 24 models) ensemble, our CMIP3 results are consistent with the study by Cook et al. (2012) and show a large consensus on increased precipitation during the wet season (Fig. 6a), and a moderate consensus on decreased precipitation during the dry season in southwest Amazonia (Fig. 6b).

Differences between CMIP3 and CMIP5 are plotted in the bottom panels. In line with Fig. 5a, the strengthening of the wet season tends to vanish in CMIP5, especially in central and eastern Amazonia, where fewer models agree on the sign of precipitation anomalies. Conversely, there is more consensus about a strengthening of the dry season, particularly in the northeast of the basin. Similar differences between CMIP5 and CMIP3 models are found in the 1 % CO_2 experiments (not shown) and are therefore not due to differences in the concentration scenarios.

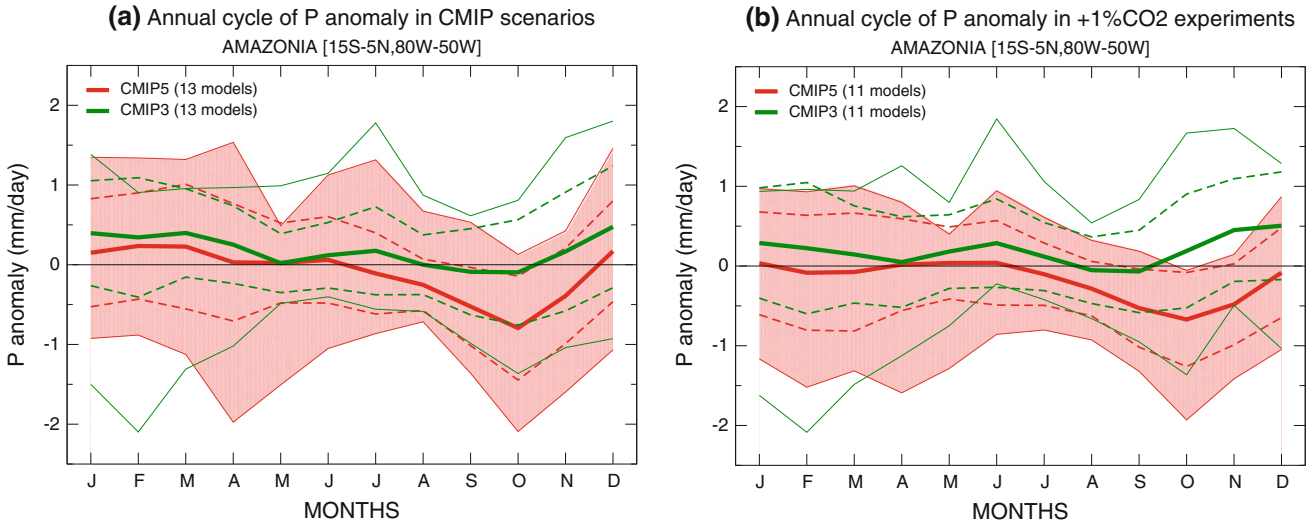

Fig. 5 CMIP5 versus CMIP3 changes in the mean annual cycle of monthly precipitation over Amazonia (absolute anomalies mm/day): **a** RCP8.5 and SRES-A2 scenarios (2071–2100 minus 1971–2000), **b** 1 % CO_2 increase experiments (years 111–140 minus years 11–40). Multi-model ensemble mean (*thick lines*) ± 1 standard deviation (*dashed lines*), as well as extreme values (*thin lines*) are shown for each ensemble. Note that only 11 out of the 13 selected models are shown in (**b**) due to the lack of 1 % CO_2 outputs for two CMIP3 models

A scatterplot of seasonal mean anomalies for individual models in CMIP3 versus CMIP5 scenarios (Fig. 7a) provides a more comprehensive picture of the uncertainties summarized in Figs. 5a and 6, where the multi-model distribution is strongly influenced by a couple of models which behave as possible "outliers". Indeed, looking at DJFM anomalies (in green), all CMIP3 simulations, except MOHC, show positive anomalies. However, looking at CMIP5 simulations, models disagree on the sign of the change for the wet season. This is partly due to the different behaviours between the eastern and western parts of the basin (Fig. 6a). Conversely, looking at the dry season (in red), there is more consensus in CMIP5 than in CMIP3. The IPSL model remains the only one projecting a wetter dry season in CMIP5 simulations. As for the ensemble mean response, it must be here emphasized that differences between the selected concentration scenarios (A2 for CMIP3 vs RCP8.5 for CMIP5) have a very limited influence on the multi-model spread. This is illustrated by Fig. 7b where CMIP5 models show a similar spread in the idealized 1 % CO_2 experiment and in the RCP8.5 climate scenario. It highlights that uncertainties in precipitation projections are dominated by model uncertainties and their sensitivity to increasing concentration of greenhouse gases.

4 Discussion

What are the possible reasons for such a shift of consensus between CMIP3/CMIP5 and the dry/wet season? A first hypothesis is that the lack of consensus about the Amazonian rainfall response, between and within the ensemble simulations, is partly related to the lack of consensus about the patterns and magnitude of tropical SST anomalies (e.g. Douville et al. 2006; Cook et al. 2012). Figure 8 indeed suggests that the regional SST response, over both the equatorial Pacific and the TNA, remains very uncertain and is not better constrained in CMIP5 versus CMIP3. While the ensemble mean shows a stronger SST warming in CMIP5, in line with the enhanced radiative forcing scenario, there are still models that project a limited surface warming over the tropical ocean. Such discrepancies are possible candidates for explaining the spread in the precipitation response. As an example (Li et al. 2011) analyzed two models (GISS-ER and UKMO-HadCM3) that predicted opposite changes over both the tropical Pacific and Atlantic oceans and consequently opposite rainfall changes over the eastern Amazon.

Looking at the global distribution of the ensemble mean SST anomalies in JJAS confirms the enhanced ocean warming in CMIP5 versus CMIP3 (Fig. 9, left panels). This feature is however more pronounced in the boreal hemisphere, both for JJAS and annual mean anomalies. This enhanced inter-hemispheric contrast could be partly responsible for the different ITCZ response between CMIP5 and CMIP3 projections (Fig. 9, right panels). While both CMIP3 and CMIP5 projections highlights enhanced zonal mean precipitation over the ITCZ, differences between CMIP5 and CMIP3 anomalies suggest an additional northward shift in the most recent scenarios. This feature is particularly clear over the tropical Atlantic and could explain to some extent the enhanced JJAS Amazonian drying found in CMIP5 projections.

Table 2 Mean length of the dry season (in number of months) for both current and future climates

Models	Threshold mm/month	CMIP3 (historical + SRES_A2)			CMIP5 (historical + RCP8.5)		
		1971–2000	2071–2100	Anomaly	1971–2000	2071–2100	Anomaly
(a) Absolute threshold							
CCCMA	100	4.4	4.0	−0.33	6.5	9.4	**2.90***
CNRM	100	2.2	2.0	−0.17	3.0	3.6	**0.53***
CSIRO	100	5.7	6.6	**0.97***	5.4	5.9	0.47
GFDL	100	6.4	6.9	0.53	5.4	5.6	0.13
GISS	100	3.0	2.5	*−0.56**	3.1	3.1	0.03
INM	100	5.4	4.6	*−0.84**	0.2	0.3	0.13
IPSL	100	4.4	3.1	*−1.30**	4.4	3.7	*−0.67**
MIROC	100	4.1	4.0	−0.13	2.2	2.5	0.30
MOHC	100	0.1	1.4	**1.30***	0.1	0.8	**0.73***
MPI	100	4.1	4.6	**0.46***	4.3	5.0	**0.77***
MRI	100	0.4	1.1	**0.67***	0.2	0.9	**0.73***
NCAR	100	3.4	3.3	−0.03	2.3	2.6	**0.33***
NCC	100	3.1	3.1	0.03	2.9	2.9	0.00
(b) Relative threshold (10th percentile calculated over 1901–2009)							
CCCMA	48	0.9	0.6	*−0.33**	1.1	4.9	**3.7***
CNRM	81	1.4	1.3	−0.17	1.2	1.7	0.50
CSIRO	48	1.3	1.2	−0.03	1.1	2.0	**0.9***
GFDL	30	1.3	2.1	0.80	1.1	1.3	0.23
GISS	69	1.1	0.2	*−0.90**	1.0	1.6	**0.60***
INM	52	1.1	0.4	*−0.70**	1.0	1.2	0.20
IPSL	43	1.1	0.2	*−0.9**	1.3	0.4	*−0.9**
MIROC	41	1.7	2.5	**0.73***	0.9	1.8	**0.97***
MOHC	127	1.4	2.6	**1.17***	1.3	3.7	**2.33***
MPI	45	1.2	2.0	**0.83***	1.5	2.2	**0.70***
MRI	113	0.8	2.1	**1.27***	1.2	2.4	**1.17***
NCAR	74	1.2	0.8	*−0.43**	1.0	1.5	0.47
NCC	44	1.1	1.0	−0.13	1.2	1.6	**0.4***

* Statistically significant anomaly at the 5 % level using a two-tailed Student *T* test

Bold values indicate positive significant anomalies

Italic values indicate negative significant anomalies

For a better understanding of this contrasted behaviour between CMIP3 and CMIP5 projections, the lower panels in Fig. 9 can be splitted into three contributions according to the following equation:

$$\begin{aligned} X^5_{RCP8.5} - X^3_{SRES-A2} = &\left(X^5_{RCP8.5} - X^5_{1\%CO_2}\right) \\ &+ \left(X^5_{1\%CO_2} - X^3_{1\%CO_2}\right) \\ &+ \left(X^3_{1\%CO_2} - X^3_{SRES-A2}\right) \end{aligned} \quad (1)$$

where X is the climatological anomaly for the selected variable (precipitation or SST), the exponent refers to the CMIP ensemble (either CMIP3 or CMIP5) and the index refers to the selected experiment (either a scenario or the idealized 1 % CO_2 experiment). Eq. (1) is particularly useful to distinguish model differences (second right-hand term) from scenario effects (first and third right hand terms).

Results are shown in Figs. 10 and 11 for JJAS precipitation and JJAS SST, respectively. As far as precipitation is concerned, the zonal mean response shown in Fig. 9 is a combination of differences in both models and radiative forcings. The model effect isolated in the 1 % CO_2 experiments (Fig. 10c) shows a "W" tripole in the tropics which might be interpreted as the impact of the increased horizontal resolution in CMIP5 models. Both model generations show a strengthening of the ITCZ in a warmer climate (Fig. 9) but the ITCZ is sharper in the

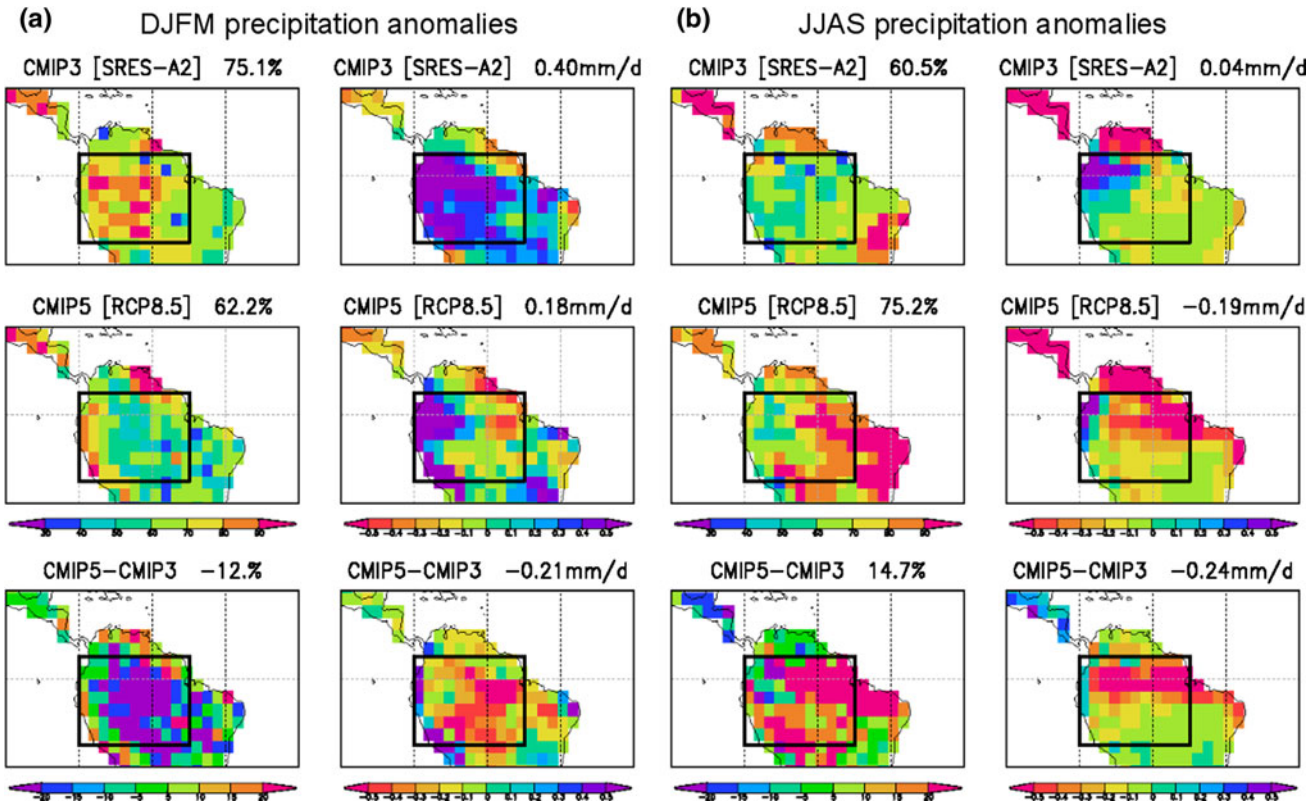

Fig. 6 CMIP5 versus CMIP3 changes (2071–2100 vs 1971–2000) in the spatial distribution of seasonal mean precipitation (mm/day), wet season (**a**) and dry season (**b**). *Left panels* model consensus (%) estimated as the percentage of models which agree on the sign of the ensemble mean change. *Right panels* ensemble mean change (mm/day). The *number* above the *right-hand corner* of each plot is the average model consensus (*left panels*) and mean P anomaly (*right panels*) over the *box outlined* in *black*

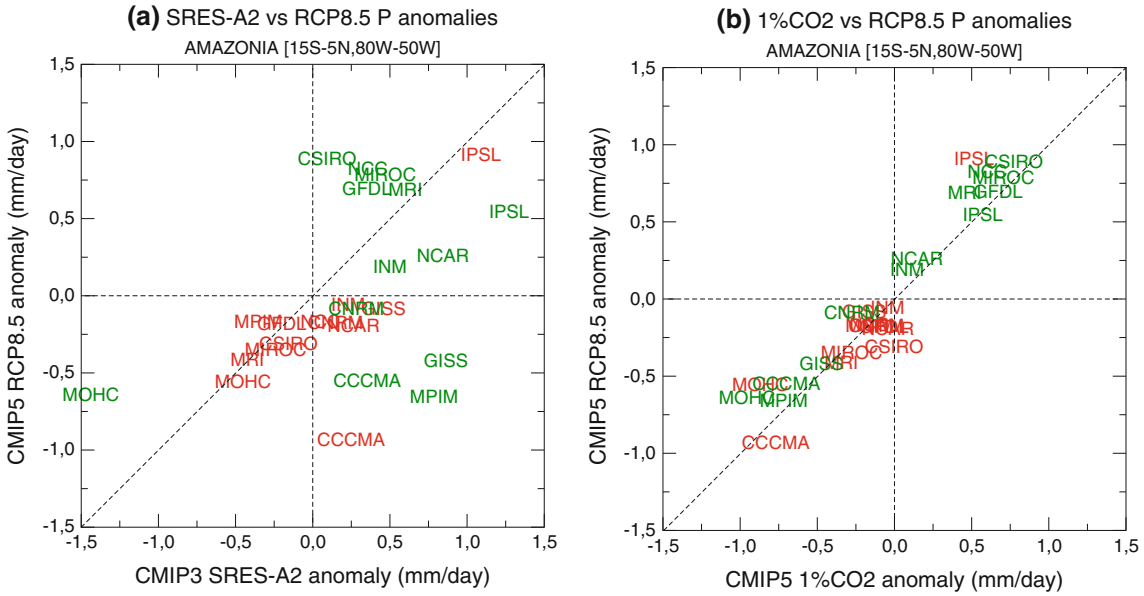

Fig. 7 Scatterplots of seasonal precipitation change (mm/day) in DJFM (*green*) and JJAS (*red*): **a** CMIP3 SRES-A2 versus CMIP5 RCP8.5 climate scenario, **b** CMIP5 1 % CO_2 increase experiment versus CMIP5 RCP8.5 climate scenario

high-resolution models so that the second right-hand term in Eq. (1) shows a tripole of negative-positive–negative zonal mean anomalies in the tropics. The other two contributions (Fig. 10b, d) indicate both a strengthening and northward shift of the ITCZ, thereby suggesting that the RCP8.5 radiative forcing is stronger and more

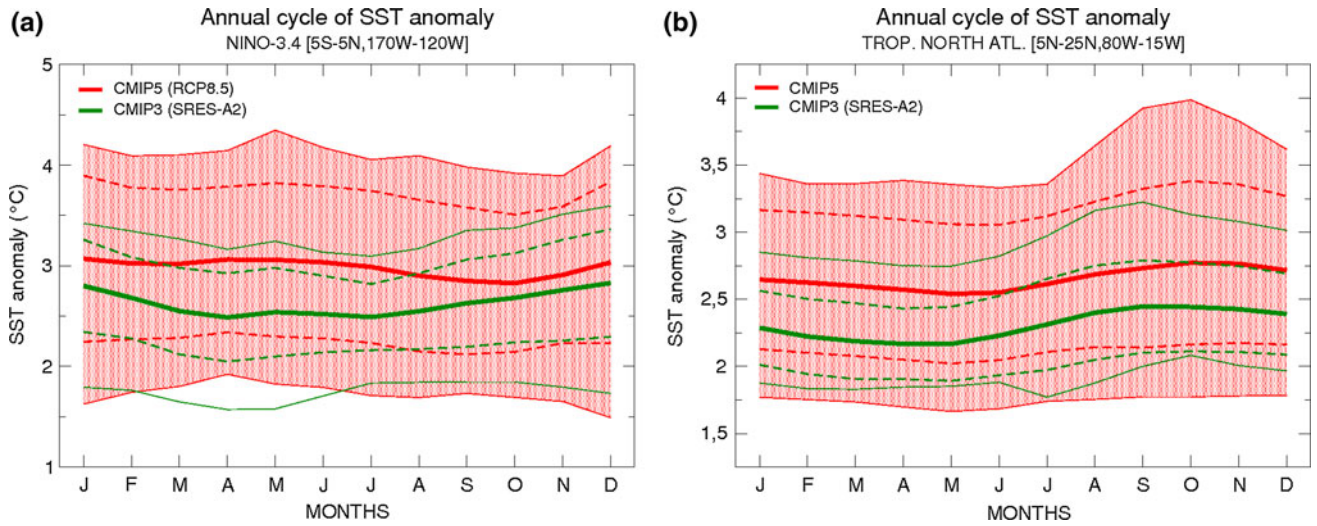

Fig. 8 CMIP5 versus CMIP3 changes (2071–2100 vs 1971–2000) in the mean annual cycle of monthly SST over **a** the equatorial Pacific and **b** the TNA: multi-model ensemble mean (*thick lines*) ± 1 standard deviation (*dashed lines*), as well as extreme values (*thin lines*)

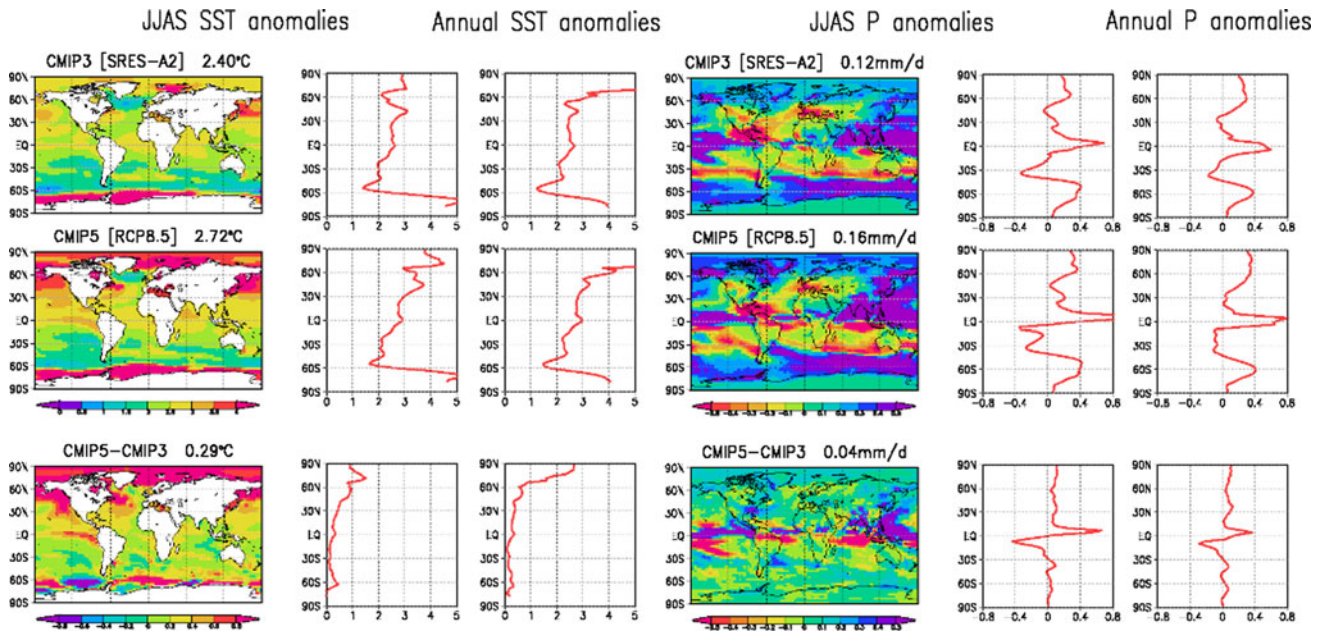

Fig. 9 Global (*left column*), zonal (*2nd column*) mean distribution of JJAS SST anomalies and zonal mean distribution of annual SST anomalies (*3rd column*) (°C), and global (*4th column*), zonal (*5th column*) mean distribution of JJAS precipitation anomalies and zonal mean distribution of annual precipitation anomalies (*6th column*) (mm/day), in (*top*) CMIP3, (*middle*) CMIP5, as well as the difference between, CMIP5 and CMIP3 (*bottom*)

asymmetric (stronger warming in the northern hemisphere) than its SRES-A2 counterpart. Such a hypothesis is confirmed by Fig. 11b and d showing an opposite latitudinal SST gradient in the tropics. In contrast, the idealized 1 % CO_2 experiments (Fig. 11c) show similar SST anomalies in the tropics between CMIP5 and CMIP3, but contrasted SST anomalies in the high latitudes partly related to an improved sea ice climatology in present-day climate (not shown).

Therefore, the different ensemble mean precipitation response between CMIP3 (SRES-A2) and CMIP5 (RCP8.5) is partly due to an increase in both horizontal resolution and in radiative forcings. The latter contribution is probably the consequence of a stronger increase in greenhouse gas concentrations in RCP8.5, but also of a stronger decline in the radiative cooling due to sulfate aerosols (Wild et al. 2005), in line with a more detailed representation of their direct and indirect effects.

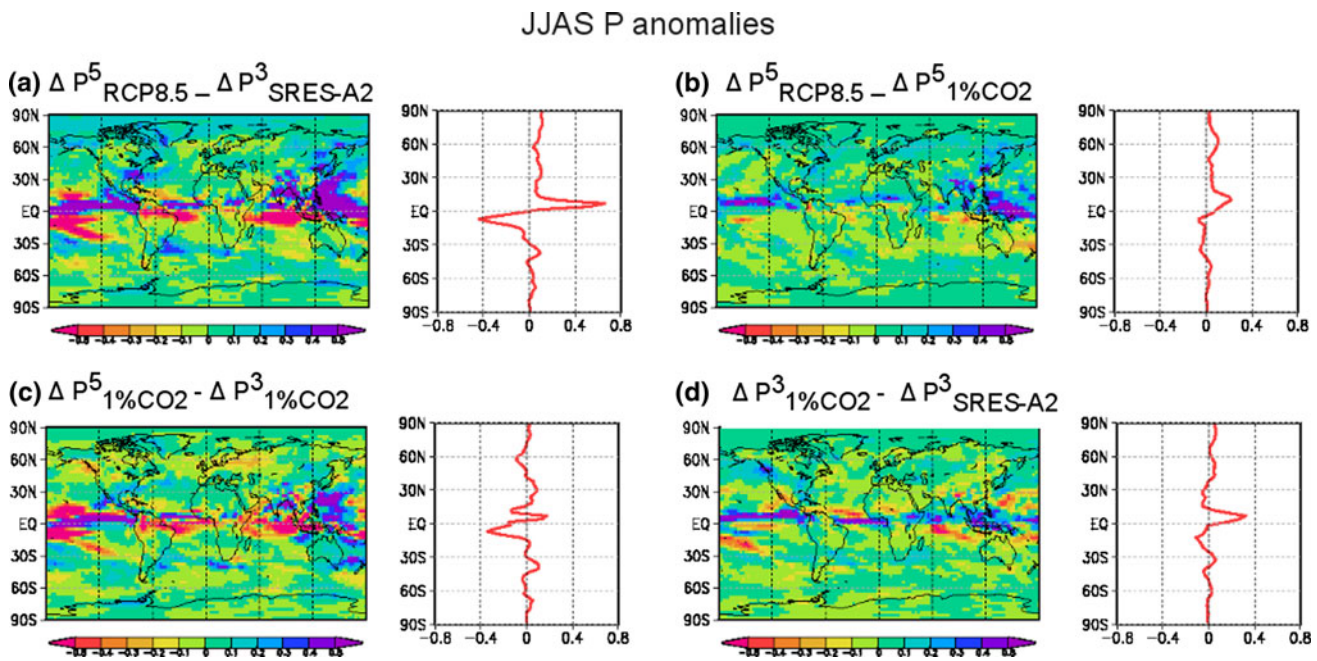

Fig. 10 Splitting of the differences between CMIP5 (RCP8.5) and CMIP3 (SRES-A2) anomalies of JJAS precipitation (mm/day) into three contributions as defined in Eq. (1) (see text for details)

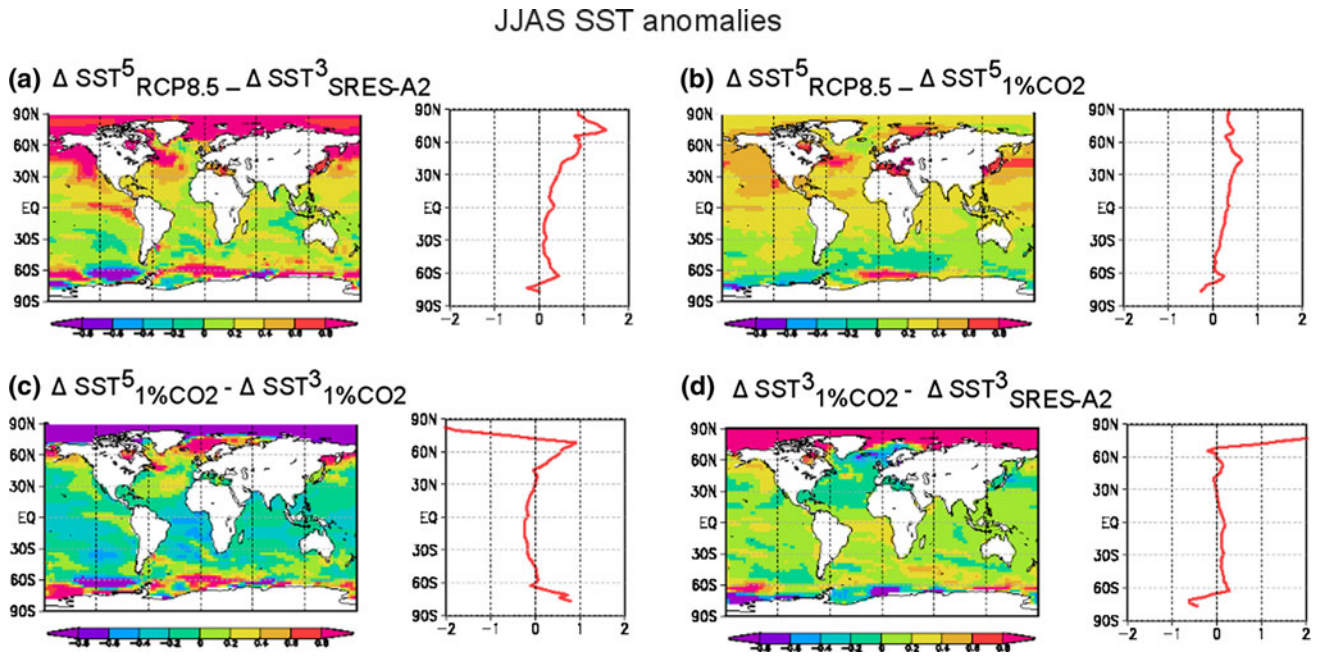

Fig. 11 Same as Fig. 10 but for JJAS SST (°C)

Beyond the zonal mean ITCZ response, regional discrepancies between CMIP3 and CMIP5 projections of JJAS precipitation over Amazonia are dominated by model differences (Fig. 10c), i.e. the second right-term in Eq. (1). The zonal mean SST response hides strong zonal asymmetries which are also important for understanding the ensemble mean precipitation response. In the 1 % CO_2 experiments (Fig. 11c), the enhanced inter-hemispheric contrast in the zonal mean SST warming is mainly found in the Atlantic basin, while differences in the tropical Pacific reveal a more pronounced El Niño-like response. In line with the improved ENSO teleconnection described in Sect.

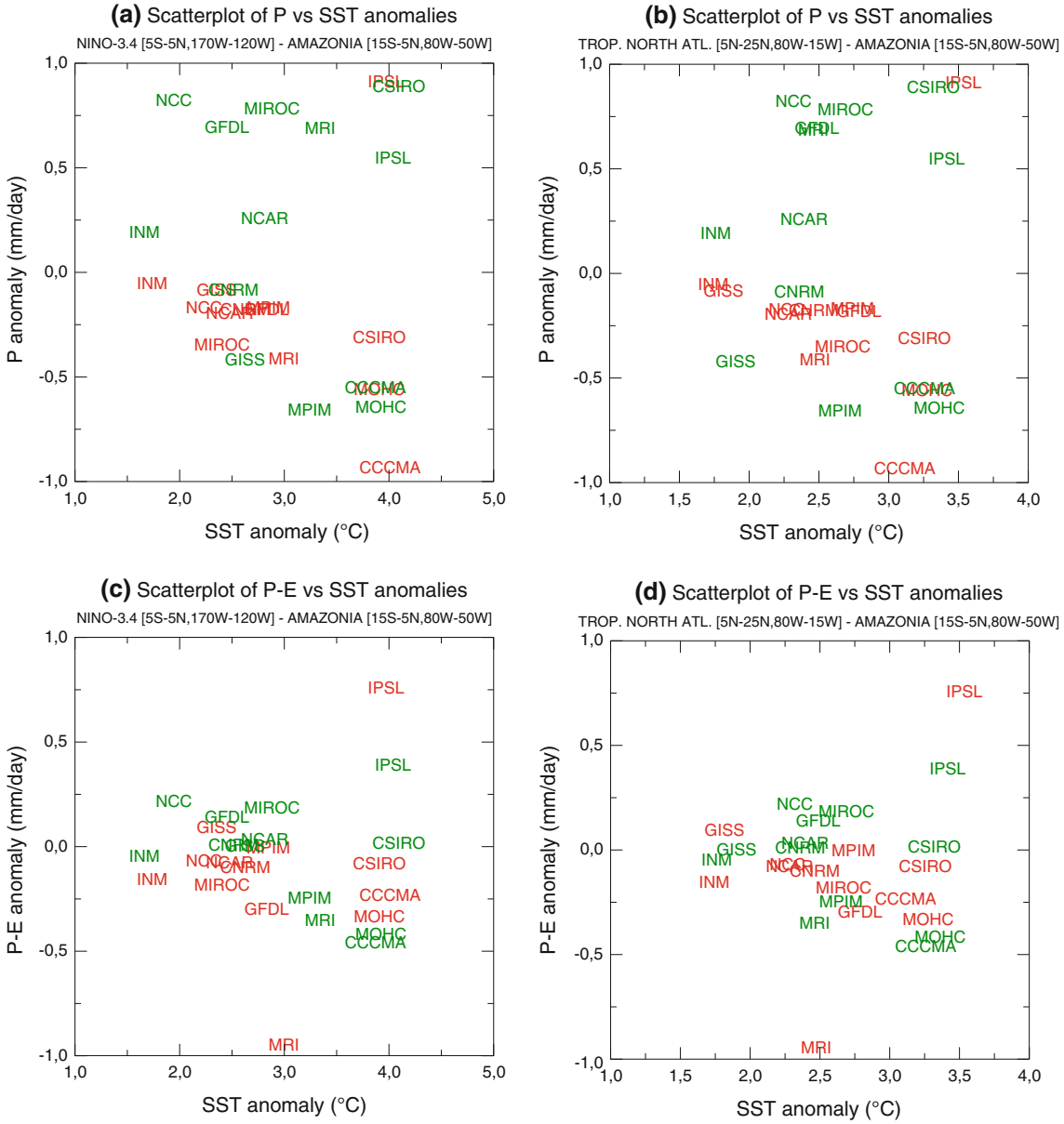

Fig. 12 Scatterplot of seasonal P (**a**, **b**) or P-E (**c**, **d**) anomalies (mm/day) over Amazonia vs seasonal SST anomalies (°C) over the Niño3.4 (**a**, **c**) or TNA (**b**, **d**) domains for CMIP5 (RCP8.5) projections. DJFM season in *green*, JJAS season in *red*

3.1, this feature which is also found in Fig. 11a could also contribute to the significant and stronger decrease in JJAS precipitation found in CMIP5 vs CMIP3 projections.

Focusing on CMIP5 projections, Fig. 12 shows scatter plots of seasonal precipitation or moisture convergence anomalies over Amazonia versus seasonal SST anomalies over the Niño3.4 or TNA domains. During the dry season (in red), the Pacific and Atlantic influence on spread in the response of Amazonian rainfall is consistent with our hypotheses about the difference between CMIP5 and CMIP3 models. Broadly speaking, the stronger the warming of the Nino-3.4 ot TNA SST is, the dryer is the response of P and P-E over Amazonia. This relationship remains however relatively fuzzy and is obviously obscured by other sources of uncertainties (e.g. the response of deep convection and/or surface evapotranspiration over Amazonia). The relationship between the precipitation and SST anomalies is even more complex during the wet season which suggests a dichotomy among CMIP5 models that is less clear for moisture convergence and is therefore mainly due to contrasted anomalies of evapotranspiration (not shown).

Moreover, the spread of the JJAS (and to lesser extent DJFM) P-E anomalies in response to SST warming is skewed by the peculiar behaviour of the IPSL model. While most models project a weaker moisture convergence

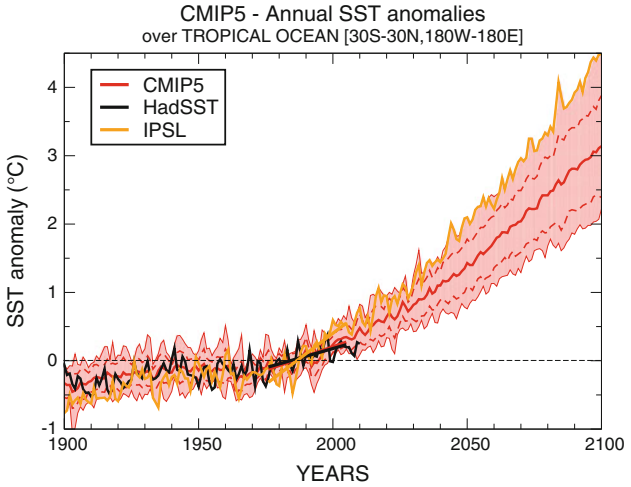

Fig. 13 Time series of monthly SST anomalies (°C) from 1850 to 2100 over the tropical ocean (30S–30N, 180W–180E) calculated over the 1971–2000 reference period: mean observed SST (HadSST *black thick line*); multi-model ensemble mean (*red thick lines*) ± 1 standard deviation (*red dashed lines*), as well as extreme values (*red thin lines*); IPLS mean (*orange thick line*)

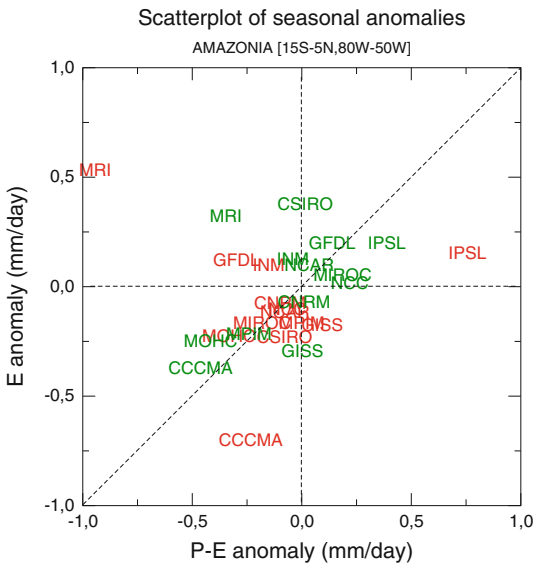

Fig. 14 Scatterplot of seasonal Amazon E anomalies (mm/day) versus P-E anomalies (mm/day) for CMIP5 (RCP8.5). DJFM (*green*) JJAS (*red*)

in the late twenty-first century, the IPSL model simulates a substantial increase of P-E (Fig. 12c), in line with the strong increase in precipitation found in Fig. 7. This could be partly explained by the unusual warming simulated over the whole tropical ocean (Fig. 13) which makes the IPSL model a possible outlier, not only among the CMIP5 models but also comparing the recent SST warming against the HadSST observations. This strong tropical SST warming can favor the increase of moisture content in the

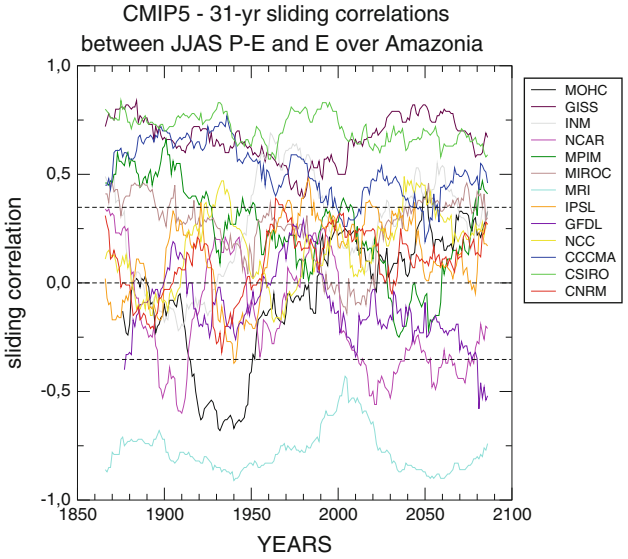

Fig. 15 Sliding correlations calculated between JJAS P-E and E over Amazonia from 1850 to 2100 over a 31-year time span for CMIP5 simulations (historical + RCP8.5)

lower atmospheric layers and drive more precipitation to the ITCZ, including over Amazonia.

Besides moisture convergence, evapotranspiration (hereafter E) is a key component of the atmospheric moisture budget as about half of rainfall falling over the Amazon basin are recycled (Cox et al. 2008), with 70 % of E coming from rainforest's transpiration (Kumagai et al. 2005). Figure 14 shows a scatterplot of the seasonal E versus P-E anomalies in CMIP5. It reveals that both E and P-E contribute to the uncertainties in the response of P, but also that a similar response in P can arise from contrasted behaviours between E and P-E, especially during the dry season. In JJAS, most models project a decrease in evapotranspiration over the Amazon basin, while four models indicate an opposite response, with the MRI and CCCMA models showing the most contrasted behaviours.

Interestingly, MRI also shows a significant anti-correlation in JJAS between moisture convergence and evapotranspiration at the interannual timescale, while other models indicate no or positive correlations (Fig. 15). Therefore, a possible reason for the atypical behaviour of this model in Fig. 14 could be a strong competition between E and P-E in this model. This could be related to the lack of soil moisture control on the dry season evapotranspiration, which could be rather driven by the incoming surface radiation. Decreased moisture convergence in this model could be associated with decreased cloudiness and thereby increased evapotranspiration. This hypothesis is consistent with the unusual wet bias found in present-day climate (Fig. 1), meaning that the dry season evaporation is indeed not necessarily limited by soil moisture in this

model. It would be interesting to compare and understand the relative influence of soil moisture and surface radiation on the response of surface evapotranspiration in our subset of CMIP5 models but this is beyond the scope of the present study.

Conversely, CCCMA shows a dramatic decrease in E despite a limited decrease in P-E in JJAS (Fig. 14). While this climate change behaviour is also fairly consistent with the E versus P-E relationship at the interannual timescale (Fig. 15), the CCCMA model is not a clear outlier in this respect. The strong evaporation decrease at the end of the twenty-first century is a direct result of the strong decrease in precipitation simulated (Fig. 7) but is also partly explained by the control of transpiration by CO_2 not present in CMIP3 (Arora et al. 2009). The new CCCMA model is indeed a fully coupled climate-carbon earth system model with a parameterization of photosynthesis including the increased stomatal control of transpiration under enhanced CO_2 concentration. Such a mechanism is however at work in other CMIP5 models and a more detailed analysis of the surface energy and water budgets would be necessary to assess its possible contribution to the inter-model spread in the response of E and P.

5 Conclusions

Significant improvements have been made from CMIP3 to CMIP5 to capture present-day precipitation over the Amazon basin. The annual mean dry bias has been consistently reduced, the spatial distribution and the seasonal cycle of rainfall is better simulated, and the inter-annual variability has also been improved in line with a better simulation of the ENSO and TNA teleconnections. Nevertheless, the twenty-first century projections remains very uncertain. The only enhanced consensus is about the strengthening and lengthening of the dry season, especially in the eastern part of the basin. This robust signal is consistent with the observed interannual variability of Amazonian precipitation and is probably due to (1) the northward shift of the ITCZ in line with an asymmetric inter-hemispheric warming of the global ocean that is particularly clear in the Atlantic basin and (2) the reinforcement of a Niño-like pattern in the equatorial Pacific. This contrasted ensemble mean response between CMIP3 and CMIP5 is also found in the idealized 1 % CO_2 experiments and is therefore due to changes in models rather than in concentration scenarios. Beyond the ensemble mean response, similar mechanisms also contribute to the inter-model spread within the CMIP5 ensemble. While such results confirm that interannual variability and teleconnections can be useful for constraining climate projections (e.g. Douville et al. 2006), other processes such as the response of evapotranspiration also contribute to the uncertainties in the projections of regional precipitation. Additional constraints on both ocean–atmosphere and land–atmosphere interactions are therefore necessary to unravel the fate of the Amazon forest and the related carbon cycle feedback in global climate projections. In this respect and as a first step, understanding the behaviour of apparent "outliers" could be more efficient than accounting for the full distribution of the models' response.

Acknowledgments The authors are grateful to Michael Coe for his helpful comments on the first draft of this article. Thanks are also due to the French Commissariat à l'Energie Atomique for supporting this study, as well as to Hervé Giordani for helpful discussion and to the anonymous reviewers for their constructive comments.

References

Arora VK, Boer GJ, Christian JR, Curry CL, Denman KL, Zahariev K, Flato GM, Scinocca JF, Merryfield WJ, Lee WG (2009) The effect of terrestrial photosynthesis down regulation on the twentieth-century carbon budget simulated with the CCCma earth system model. J Clim 22:6066–6088

Betts RA, Cox PM, Collins M, Harris PP, Huntingford C, Jones CD (2004) The role of ecosystem–atmosphere interactions in simulated Amazonian precipitation decrease and forest die-back under global climate warming. Theor Appl Climatol 78:157–175. doi:10.1007/s00704-004-0050-y

Botta A, Ramankuttym N, Foley JA (2002) Long-term variations of climate and carbon fluxes over the Amazon Basin. Geophys Res Lett 29:564–579

Bretherton CS, Smith C, Wallace M (1992) An intercomparison of methods for finding coupled patterns in climate data. J Clim 5:541–560

Cook B, Zeng N, Yoon J-H (2012) Will Amazonia dry out? Magnitude and causes of change from IPCC climate model projections. Earth Interact 16:1–27

Cox PM, Betts RA, Jones CD, Spall SA, Totterdell IJ (2000) Acceleration of global warming due to carbon-cycle feedbacks in a coupled climate model. Nature 408:184–187. doi:10.1038/35041539

Cox PM, Betts RA, Collins M, Harris PP, Huntingford C, Jones CD (2004) Amazonian forest die-back under climate-carbon cycle projections for the 21st century. Theor Appl Climatol 78:137–156. doi:10.1007/s00704-004-0049-4

Cox PM, Harris PP, Huntingford C, Betts RA, Collins M, Jones CD, Jupp TE, Marengo JA, Nobre CA (2008) Increasing risk of Amazonian drought due to decreasing aerosol pollution. Nature 453:212–215

Dai A (2006) Precipitation characteristics in eighteen coupled climate models. J Clim 19(18):4605–4630

Douville H, Salas-Mélia D, Tyteca S (2006) On the tropical origin of uncertainties in the global land precipitation response to global warming. Clim Dyn 26:367–385. doi:10.1007/s00382-005-0088-2

Douville H, Decharme B, Ribes A, Alkama R, Sheffield J (2012) Anthropogenic influence on multi-decadal changes in reconstructed global evapotranspiration. Nat Clim Change. doi:10.1038/NCLIMATE1632

Foley JA (2002) El Niño–Southern oscillation and the climate, ecosystems and rivers of Amazonia. Global Biogeochem Cycles 16:1132. doi:10.1029/2002GB001872

Foley JA, Costa MH, Delire C, Ramankutty N, Snyder P (2003) Green surprise: howterrestrial ecosystems could affect Earth's climate. Front Ecol Environ 1:38–44

Good P, Jones C, Lowe J, Betts R, Gedney N (2012). Comparing tropical forest projections from two generations of Hadley Centre Earth System models, HadGEM2-ES and HadCM3LC. J Clim. doi:10.1175/JCLI-D-11-00366.1

Joetzjer E, Douville H, Delire C, Ciais P, Decharme B, Tyteca S (2012) Evaluation of drought indices at interannual to climate change timescales: a case study over the Amazon and Mississippi river basins. Hydrol Earth Syst Sci Discuss 9:13231–13249. doi:10.5194/hessd-9-13231-2012

Kumagai TO, Saitoh TM, Sato Y, Takahashi H, Manfroi OJ, Morooka T, Kuraji K, Suzuki M, Yasunari T, Komatsu H (2005) Annual water balance and seasonality of evapotranspira- tion in a Bornean tropical rainforest. Agric For Meteorol 128:81–92

Lewis SL, Brando PM, Phillips OL, Van Der Heijden GMF, Nepstad D (2011) The 2010 Amazon drought. Science 331:554

Li W, Fu R, Dickinson RE (2006) Rainfall and its seasonality over the Amazon in the 21st century as assessed by the coupled models for the IPCC AR4. J Geophys Res 111:1–14

Li W, Zhang P, Ye J, Li L, Backer PA (2011) Impact of two different types of El Nino events on the Amazon climate and ecosystem productivity. J Plant Ecol 4(1–2):91–99. doi:10.1093/jpe/rtq039

Malhi Y, Roberts JT, Betts RA, Killeen TJ, Li W, Nobre CA (2008) Climate change, deforestation, and the fate of the Amazon. Science 319:169–172. doi:10.1126/science.1146961

Malhi Y et al (2009) Exploring the likelihood and mechanism of a climate-change-induced dieback of the Amazon rainforest. Proc Natl Acad Sci USA 106(49):20610–20615

Marengo JA (1992) Interannual variability of surface climate in the Amazon basin. Int J Climatol 12:853–863

Marengo JA (2004) Interdecadal variability and trends of rainfall across the Amazon basin. Theor Appl Climatol 78(1–3):79–96. doi:10.1007/s00704-004-0045-8. http://springerlink.metapress.com/openurl.asp?genre=article&id

Marengo JA et al (2008) The drought of Amazonia in 2005. J Clim 21(3):495–516

Marengo JA, Tomasella J, Alves LM, Soares WR, Rodriguez DA (2011) The drought of 2010 in the context of historical droughts in the Amazon region. Geophys Res Lett 38:1–5. doi:10.1029/2011GL047436

Meggers B (1994) Archeological evidence for the impact of Mega-El Niño events on Amazonia during the past two millennia. Clim Change 28:321–338

Phillips O, Aragão L, Lewis S et al (2009) Drought sensitivity of the Amazon rainforest. Science (New York, N.Y.) 323(5919): 1344–1347

Potter C, Klooster S, Hiatt C, Genovese V, Castilla-Rubio JC (2011) Changes in the carbon cycle of Amazon ecosystems during the 2010 drought. Environ Res Lett 6:034024

Power SB, Delage F, Colman R, Moise A (2012) Consensus on twenty-first century rainfall projections in climate models more widespread than previously thought? J. Climate 25:3792–3809

Rammig A, Jupp T, Tietjen B, Heinke J, Ostberg S, Cox PM (2010) Estimating the risk of Amazonian forest dieback. New Phytol 187:695–707

Rayner NA, Parker DE, Horton EB, Folland CK, Alexander LV, Rowell DP, Kent EC, Kaplan A (2003) Global analyses of sea surface temperature, sea ice, and night marine air temperature since the late nineteenth century. J Geophys Res 108(14):4407. doi:101029/2002JD002670

Riahi K, Gruebler A, Nakicenovic N (2007) Scenarios of long-term socio-economic and environmental development under climate stabilization. Technol Forecast Soc Chang 74(7):887–935

Riahi K et al (2011) RCP 8.5 A scenario of comparatively high greenhouse gas emissions. Clim Change 109(1–2):33–57

Richey J, Nobre CA, Deser C (1989) Amazon River discharge and climate variability: 1903 to 1985. Science 246:101–103

Richter I, Xie SP, Wittenberg AT, Masumoto Y (2012) Tropical Atlantic biases and their relation to surface wind stress and terrestrial precipitation. Clim Dyn 38:985–1001

Rojas M, Seth A, Rauscher SA (2006) Relationship between precipitation and moisture flux changes in the SRES A2 scenario for the South American monsoon region. CLARIS News 3:14–20

Rudolf B et al (2011) New GPCC full data reanalysis version 5 provides high-quality gridded monthly precipitation data. GEWEX News 21(2):4–5

Seager R, Naik N, Vecchi G (2010) Thermodynamic and dynamic mechanisms for large-scale changes in the hydrological cycle in response to global warming. J Clim 23:4651–4668

Sellers PJ, Bounoua L, Collatz GJ, Randall DA, Dazlich DA, Los SO, Berry JA, Fung I, Tucker CJ, Field CB, Jensen TG (1996) Comparison of radiative and physiological effects of doubled atmospheric CO2 on climate. Science 271:1402–1406. doi:10.1126/science.271.5254.1402

Sombroek W (2001) Spatial and temporal patterns of amazon rainfall. Consequences for the planning of agricultural occupation and the protection of primary forests. Ambio 30:388–396

Uvo CRB, Repelli CA, Zebiak S, Kushnir Y (1998) The relationship between tropical Pacific and Atlantic SST and Northeast Brazil monthly precipitation. J Clim 11:551–562

Vera C et al (2006) Climate change scenarios for seasonal precipitation in South America from IPCC-AR4 models. Geophys Res Lett 33(13):2–5

Wallace JM, Lim GH, Blackmon ML (1988) Relationship between cyclone tracks, anticyclone tracks and baroclinic waveguides. J Atmos Sci 45:439–462

Wallace JM, Smith C, Bretherton CS (1992) Singular value decomposition of Wintertime Sea surface temperature and 500-mb height anomalies. J Clim 5:561–576

Wild M et al (2005) From dimming to brightening: decadal changes in solar radiation at earth's surface. Science 308:847–850. doi:10.1126/science.1103215

Xu L, Samanta A, Costa M, Ganguly S, Nemani R, Myeni R (2011) Widespread decline in greenness of Amazonian vegetation due to the 2010 drought. Geophys Res Lett 38(7):2–5

Yoon JH, Zeng N (2009) An Atlantic influence on Amazon rainfall. Clim Dyn 34:249–264

Zeng N (1999) Seasonal cycle and interannual variability in the Amazon hydrologic cycle. J Geophys Res 104:9097–9106

Zeng N, Yoon JH, Marengo JA, Subramaniam A, Nobre CA, Mariotti A, Neelin JD (2008) Causes and impacts of the 2005 Amazon drought. Environ Res Lett 3:014002